Article

Chemistry & Biology

Host-Microbe Protein Interactions during Bacterial Infection

Graphical Abstract

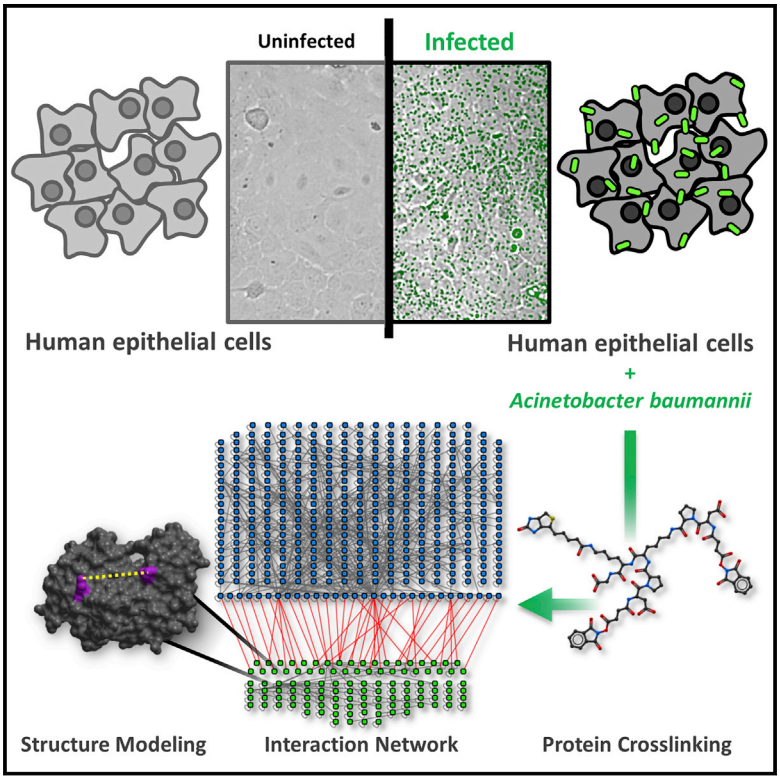

Highlights

- 3,076 crosslinked peptide pairs identified from infected cells
- 46 interspecies protein-protein interactions were identified from cells
- Interspecies interactions involving unannotated *A. baumannii* proteins were identified
- Structural features of OmpA-desmoplakin interaction revealed

Authors

Devin K. Schweppe, Christopher Harding, Juan D. Chavez, ..., Pradeep K. Singh, Colin Manoil, James E. Bruce

Correspondence

jimbruce@u.washington.edu

In Brief

Pathogenic bacteria exploit host resources through difficult-to-determine interactions between bacterial and host proteins. Schweppe et al. identified interspecies protein interactions during *Acinetobacter baumannii* infection of lung epithelia by protein crosslinking and mass spectrometry. Host protein targets for bacterial virulence factors were revealed, and crosslinked sites provide structural information for interspecies interactions during infection.

Schweppe et al., 2015, Chemistry & Biology *22*, 1521–1530
November 19, 2015
http://dx.doi.org/10.1016/j.chembiol.2015.09.015

Chemistry & Biology
Article

Host-Microbe Protein Interactions during Bacterial Infection

Devin K. Schweppe,[1] Christopher Harding,[2] Juan D. Chavez,[1] Xia Wu,[1] Elizabeth Ramage,[1] Pradeep K. Singh,[2] Colin Manoil,[1] and James E. Bruce[1,2,3,*]
[1]Department of Genome Sciences, University of Washington School of Medicine, Seattle, WA 98195, USA
[2]Departments of Medicine and Microbiology, University of Washington School of Medicine, Seattle, WA 98195, USA
[3]Department of Genome Sciences, University of Washington School of Medicine, 850 Republican Street, Brotman Building, Room 154, Seattle, WA 98109, USA
*Correspondence: jimbruce@u.washington.edu
http://dx.doi.org/10.1016/j.chembiol.2015.09.015

SUMMARY

Interspecies protein-protein interactions are essential mediators of infection. While bacterial proteins required for host cell invasion and infection can be identified through bacterial mutant library screens, information about host target proteins and interspecies complex structures has been more difficult to acquire. Using an unbiased chemical crosslinking/mass spectrometry approach, we identified interspecies protein-protein interactions in human lung epithelial cells infected with *Acinetobacter baumannii*. These efforts resulted in identification of 3,076 crosslinked peptide pairs and 46 interspecies protein-protein interactions. Most notably, the key *A. baumannii* virulence factor, OmpA, was identified as crosslinked to host proteins involved in desmosomes, specialized structures that mediate host cell-to-cell adhesion. Co-immunoprecipitation and transposon mutant experiments were used to verify these interactions and demonstrate relevance for host cell invasion and acute murine lung infection. These results shed new light on *A. baumannii*-host protein interactions and their structural features, and the presented approach is generally applicable to other systems.

INTRODUCTION

Interspecies protein interactions and the underlying structural interfaces are essential for bacterial infection. The molecular-level arms race between hosts and pathogens is carried out on multiple fronts, but predominantly takes place through evolutionary adaptation of protein structural landscapes (Elde et al., 2009; Elde and Malik, 2009; Demogines et al., 2013; Barber and Elde, 2014; Patel et al., 2012). Bacteria commandeer host resources through evolutionarily optimized bacterial protein structures that bind with high specificity to host protein cognates. Pathogen proteins target diverse host proteins involved in metabolite acquisition (Barber and Elde, 2014), molecular trafficking to the cell membrane (Elde and Malik, 2009), cytoskeletal rearrangement (Cossart and Lecuit, 1998), and cell-adherence complexes (Okuda et al., 2010). As an example, iron is necessary for biochemical processes in both bacteria and hosts, and can be sequestered by the vertebrate membrane protein transferrin to defend against bacterial infection (Barber and Elde, 2014; Zarantonelli et al., 2007). In response, bacteria such as *Neisseria gonorrhoeae* and *Haemophilus influenzae* have evolved transferrin-binding proteins (TbpA) capable of binding and scavenging iron directly from transferrin to overcome sequestration (Zarantonelli et al., 2007). Barber and Elde (2014) showed that single point mutations in transferrin alter TbpA affinity at the interface of the two proteins and are responsible for establishing the host range of the bacteria and modulating host nutritional immunity. Therefore, knowledge of not only the proteins involved in host-pathogen protein interactions but also the manner of their interaction, i.e. structural insight into interfacial regions, can profoundly advance understanding of bacterial infection and provide insight for the development of new antimicrobial therapies (Barber and Elde, 2014).

Technologies have evolved to allow large-scale protein interaction identification, but relevant information on host-pathogen interspecies interactions and structures is still limited. Two-hybrid (Fields and Song, 1989), affinity purification mass spectrometry (MS) (Sowa et al., 2009) and protein complement (Tarassov et al., 2008) methods have made the large-scale study of protein-protein interactions (PPIs) possible. Although recent efforts with these techniques have demonstrated the ability to identify PPIs relevant to host-pathogen interactions, including the virus-human protein interactions of HIV (Jager et al., 2012) and H1N1 (Shapira et al., 2009), host-pathogen PPIs remain a general challenge to identify. Furthermore, structural details pertaining to host-pathogen protein interactions are exceedingly sparse. Many aspects of host-pathogen interactions are mediated by membrane proteins, as exemplified by the transferrin case above. With roles in quorum sensing, secretion, adhesion, and invasion, membrane proteins play pivotal roles in bacterial pathogenesis, yet they often require significant dedicated efforts for interaction studies, are less suitable for many large-scale methods, and are equally challenging for conventional structural characterization (Carpenter et al., 2008).

Alternative technologies have the potential to shed light on interspecies PPIs and their structural interfaces. Chemical crosslinking MS (XL-MS) approaches are beginning to have a greater impact on protein interaction studies (Tang et al., 2005; Herzog et al., 2012; Gingras et al., 2007; Petrotchenko and Borchers, 2010; Yang et al., 2012; Tosi et al., 2013). Because of the finite

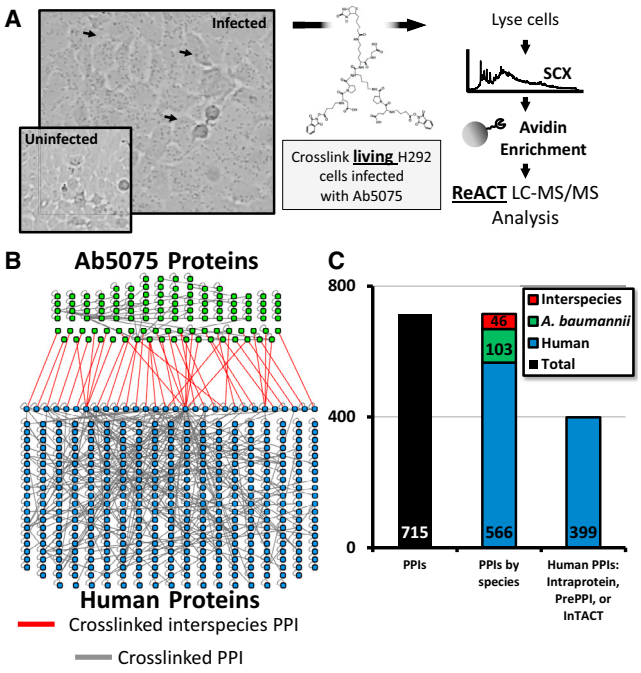

Figure 1. Identification of Protein Interactions from Infected Lung Epithelial Cells

(A) H292 cells were infected with Ab5075, crosslinked using BDP-NHP. Digested peptides were enriched and analyzed by liquid chromatography-tandem MS (LC-MS/MS). Arrows highlight individual bacteria. SCX, strong cation exchange.

(B) PPI map of human (blue) and bacterial (green) proteins. Interspecies crosslinks are highlighted in red.

(C) Total number of PPIs within the dataset, their breakdown by species (human-human, Ab5075-Ab5075, or Ab5075-human), and the relative matched interactions from orthogonal data (i.e. previously observed in PrePPI [Zhang et al., 2013]/IntAct [Orchard et al., 2014] or intraprotein PPIs within a single protein).

crosslinker length, covalent linkage of two amino acid side chains indicates their proximity during the crosslinking reaction period. Identification of crosslinked peptide pairs provides useful distance constraints for development and assessment of structural models, as illustrated for the interactions of protein in purified complexes from the protein phosphatase 2A network (Herzog et al., 2012). Chemical crosslinking can be carried out with mixtures of proteins in cell lysates (Yang et al., 2012; Rinner et al., 2008; Subbotin and Chait, 2014) or on living cells (Zhang et al., 2009; Tang et al., 2007; Kaake et al., 2014), whereby interaction identification and structural details on complexes can be performed in an unbiased manner (Chavez et al., 2011; Navare et al., 2015; Weisbrod et al., 2013; Zheng et al., 2013). This approach holds great potential for the determination of transient or long-lived interactions that have been chemically stabilized (Subbotin and Chait, 2014), particularly for the identification of protein interactors and structural details of membrane proteins (Navare et al., 2015). For example, the outer membrane protein OmpA in *Escherichia coli* is important for adhesion to host cells, catheters, and implants among its other roles (Confer and Ayalew, 2013). OmpA has been among the most heavily studied bacterial membrane proteins over the past 30 or more years. However, the protein was only recently shown to exist as a multimer through in vivo crosslinked sites within its C-terminal domain (Zheng et al., 2011). This finding was recently verified in vitro by site-directed mutation based on our reported crosslinked sites and native MS measurements (Marcoux et al., 2014). Our recent efforts have further shown that in vivo crosslinking can yield large-scale interactions and structural details on complexes in pathogenic bacterial cells, such as *Pseudomonas aeruginosa* (Navare et al., 2015). These results demonstrated that OprF, an OmpA-homolog in *P. aeruginosa*, exists as a multimer in vivo. In addition, these data showed the potential to gain information from living cells on the interactions and structures of membrane and soluble protein complexes in systems where molecular biology-based strategies are less developed or even unsuitable.

Given the unbiased capabilities for membrane protein interactions and structural characterization, chemical crosslinking technologies offer the potential for identification of interspecies interactions that can help increase our understanding of bacterial infection. The results presented here illustrate the initial crosslinking application of protein interaction reporter (PIR) technologies to the study of interspecies PPIs in human lung epithelial cells infected with the nosocomial pathogen, *A. baumannii*. These efforts produced the first large-scale interspecies crosslink dataset, including 46 host-pathogen PPIs, several of which involve the key *A. baumannii* virulence factor OmpA.

RESULTS

Determination of Interspecies Protein Interactions

In vivo proteomic XL-MS analysis of proteins from infected lung epithelial cells generated 16,758 crosslinked peptide-peptide relationships (Figure 1A). Of these we identified 3,076 non-redundant peptide-peptide relationships across three biological replicates at a relationship false discovery rate (FDR) of 0.24% (Table S1). Crosslinked peptide-peptide relationships were mapped to a network of 715 PPIs attributed to 488 human proteins and 113 bacterial proteins (Figures 1B, 1C, and S1). Identified human proteins covered an abundance range of greater than five orders of magnitude (Figure S1C) (Beck et al., 2011). Relationships between two peptides from the same protein constituted the majority of identifications (intraprotein PPIs). Two residues within a single protein have a high likelihood of being in close physical contact within a cell, are therefore more frequently crosslinked, and make up a higher proportion of interactions in crosslinked datasets (Subbotin and Chait, 2014; Zybailov et al., 2013). Importantly, intraprotein interactions define proximal residues within a protein, and thereby provide valuable structural coordinates for identified proteins even when no known structure exists for this protein (Figure 2). Alternatively, interprotein PPIs were derived from crosslinked relationships between peptides from two different proteins. Interprotein PPIs were used to generate interaction networks (Figures 1B and 3) and yielded structural data pertaining to the interaction interfaces of protein complexes. Within the interprotein relationships, we determined that 3.7% of the total peptide-peptide crosslinks, and 6.4% of all PPIs, were interspecies interactions (Figures 1B and 1C). No bacterial proteins or interspecies interactions were detected in uninfected, crosslinked H292 cells (Table S2). Based on these

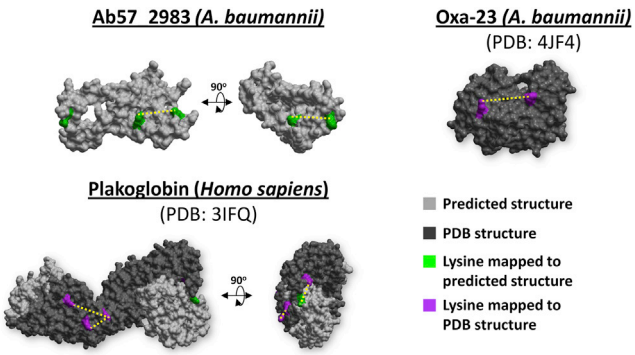

Figure 2. Intraprotein Interactions Mapped to Known and Predicted Protein Structures

Crosslinked sites identified in the large-scale proteomic infection experiment were mapped to Phyre2 predicted structures (Kelley and Sternberg, 2009) (green lysine sites, light gray model) or known crystal structures (magenta lysine sites, dark gray model) for the bacterial proteins Ab57_2983 and Oxa23 and the human protein plakoglobin. For plakoglobin, while the central domain has been crystallized (PDB: 3IFQ) the N- and C-terminal portions have not been crystallized, yet a site within the C terminus was identified in an intraprotein crosslinked relationship and is shown within the predicted structural model of this region.

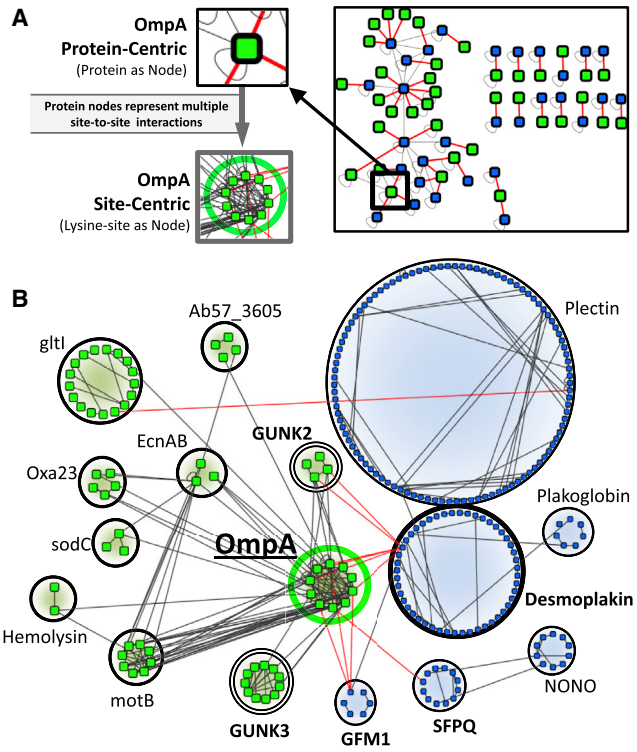

Figure 3. Depth of Interspecies and OmpA-Specific Intercellular Interactions

(A) Force-directed network of the interspecies protein interactions identified between *A. baumannii* and human proteins. Insets depict how multiple site-to-site crosslink interactions underlie each PPI. Interspecies crosslinks are shown in red.

(B) Site-to-site interactions for all proteins (bacterial and human) interacting with OmpA in the cell infection model. Nodes are individual lysine sites identified in crosslinked relationships between human (blue nodes) and bacterial (green nodes) proteins. Interspecies links are shown in red.

crosslinked relationships we constructed a protein interaction network that included host-host, pathogen-pathogen, and host-pathogen PPIs (Figure 1B).

To verify that PIR technology could detect physiological protein complexes and interactions, we quantified the number of human PPIs that were (1) intraprotein interactions or (2) were previously annotated in a PPI database (i.e. PrePPI [Zhang et al., 2013] and IntAct [Orchard et al., 2014]). Of 566 unique human PPIs, 70% were attributed to either intraprotein interactions or identified in a PPI database (Figure 1C). Subnetworks of PPIs from known complexes included host cytoskeleton, heterogeneous ribonucleoproteins, integrins, histones, cohesin, and ATP synthase (Figure S2) (Franceschini et al., 2013). Identified *A. baumannii* PPIs included interactions with virulence factors, membrane integrity proteins, metabolic complexes, transcription and translation machinery, and many genes of unknown function (GUNKs) (Table S1). The last group represents a large, and potentially important, subset of the *A. baumannii* proteome. Although they make up approximately 30% of all the *A. baumannii* proteins (Figure S1D), functional characterization of GUNK proteins is a challenge (Meier et al., 2013). Owing to structural and network information derived from identified crosslinked peptide relationships, this work provides insight into functional roles for several GUNK proteins.

A. baumannii Interactions with Host Proteins

Bacterial adherence and internalization require host-microbe protein interactions involving bacterial virulence factors binding host signaling complexes, host membrane adherence proteins, and host cytoskeletal proteins (Okuda et al., 2010; Cossart and Sansonetti, 2004; Swanson and Baer, 1995). Bacterial membrane proteins and proteins secreted via outer membrane vesicles (OMVs) were previously suggested to be a major mechanism by which *A. baumannii* adhere to host cells (Choi et al., 2008a) and deliver effector molecules (Kwon et al., 2009). Interestingly, the bacterial proteins observed in interspecies PPIs were enriched for the presence of predicted signal peptides ($p = 0.019$) (Petersen et al., 2011) and proteins observed in OMVs ($p = 0.026$) (Kwon et al., 2009) (Figure S1E). Furthermore, we observed crosslinked relationships involving bacterial proteins previously determined to be *A. baumannii* virulence factors, including OmpA, Lon protease, Oxa-23, hemolysin, TolB, TonB, and several lipoproteins (Figure 3 and Table S1) (McConnell et al., 2013). We found crosslinked relationships between several of these virulence factors (lipoproteins, OmpA, and Lon protease) and human proteins from the cytoskeleton (keratin-7, keratin-8, keratin-18, actin B, plectin, Arp 2/3-1B) and junctional adherence proteins (desmoplakin [DSP], plakoglobin, plectin) (Figure 3B) (Swanson and Baer, 1995; Choi et al., 2008a; Delva et al., 2009).

Verification of OmpA as an Essential Virulence Factor in Ab5075

Interactions identified between OmpA and host or bacterial proteins were of special interest, as OmpA orthologs in other bacteria and *A. baumannii* strains are necessary for bacterial invasion

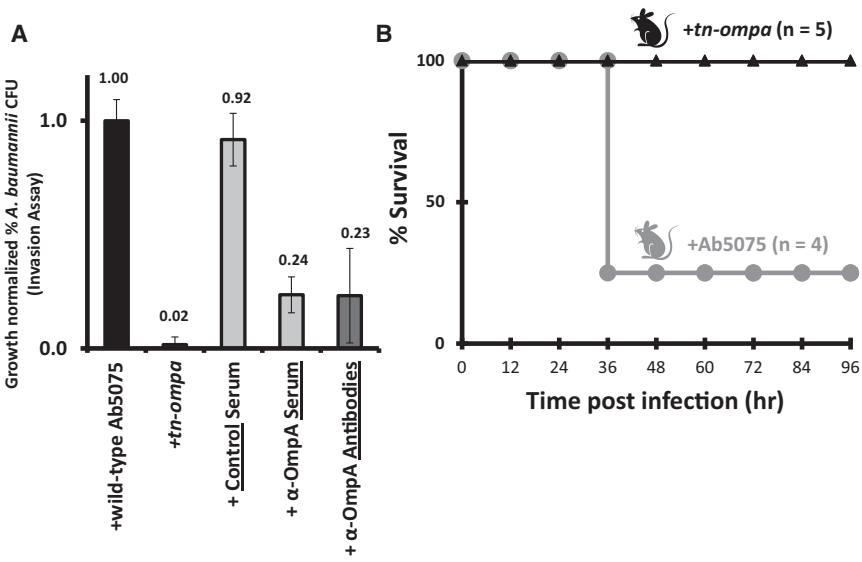

Figure 4. OmpA-Related Virulence in Ab5075

(A) Ab5075 invasion assays comparing WT Ab5075, Ab5075 with transposon disruption of OmpA (*tn-ompA*), and WT Ab5075 treated with control immunoglobulin G serum, α-OmpA serum, or purified α-OmpA antibodies. Mean ± SEM.

(B) Murine intratracheal infection with WT Ab5075 (gray) or *tn-ompa* (black, log-rank p = 0.025).

(Confer and Ayalew, 2013; Choi et al., 2008a). We needed to verify this critical role of OmpA in Ab5075 to better understand the significance of the in vivo crosslinking results and establish the pathogenic characteristics of this clinical isolate (Jacobs et al., 2014). To investigate the role of OmpA in the *A. baumannii* strain Ab5075, we first tested bacterial invasion of a gene inactivation mutant of OmpA (transposon insertion, *tn-ompa*) in the Ab5075 genetic background. Invasion of host cells was severely attenuated for the *tn-ompa* mutant compared with wild-type Ab5075 (WT, Figures 4A and S3A). Second, pre-treatment with α-OmpA serum prior to infection significantly attenuated Ab5075's ability to invade host cells (Figure 4A). Third, we quantified bacterial invasion after pre-treatment of bacterial cells with novel, purified, and targeted OmpA antibodies (Figures 4A and S3B). Three antibodies, targeting two extracellular loops and a C-terminal portion of OmpA, were generated and pooled (Figure S3B). We observed that these targeted antibodies were able to attenuate bacterial invasion to the same degree as α-OmpA serum (Figure 4A). Finally, in an acute murine lung infection model, all five mice treated with *tn-ompa* survived bacterial challenge, while three of the four mice treated with WT Ab5075 succumbed to infection within 36 hr (Figure 4B). Taken together, these findings establish the significance of OmpA in Ab5075 virulence and highlight new tools for studying Ab5075 virulence (i.e. *tn-ompa* strain and targeted antibodies).

Identification of Interactions between a Host Desmosome and *A. baumannii* Proteins

Bacterial outer membrane proteins have been proposed to be involved in host cell adherence and evasion of host immunity (Galdiero et al., 2012), and the outer membrane protein OmpA appears critical in several bacterial species (Confer and Ayalew, 2013; Choi et al., 2008a). Therefore, identification of OmpA crosslinked to several host proteins in infected cells, including an obligate component of desmosomes and hemi-desmosomes (Figure 3B), offers new insight into OmpA function during cell invasion. Peptide sequences from DSP and OmpA were unique to the human and *A. baumannii* proteomes, respectively (Table S1).

Bacterial infiltration of host epithelial layers has been demonstrated to involve close proximal relationships between desmosomes and bacterial cells (van Schilfgaarde et al., 1995). Desmosomes are cell-adhesion complexes that mediate cell-to-cell contact in host epithelia (Delva et al., 2009; Nekrasova and Green, 2013; Garrod and Chidgey, 2008), and—along with tight junctions, gap junctions, and adherens junctions—create a physical barrier to prevent bacterial intrusion through the epithelium (Lievin-Le Moal and Servin, 2006). DSP-OmpA crosslinked peptides that we identified correspond to sites within the C termini of both proteins. Disruption of the DSP C terminus has been reported to interfere with epithelial integrity (Garrod and Chidgey, 2008); therefore, virulence factor binding the DSP C terminus could serve to destabilize host cell-to-cell interactions to bypass the barrier function of host epithelia (Peterson and Artis, 2014). Sites of crosslinking within both proteins were mapped to C-terminal crystal structures of OmpA and DSP (PDB: 4G4Y [OmpA] and 1LM5 [DSP]; Choi et al., 2002; Park et al., 2012) (Figure 5A) (Schneidman-Duhovny et al., 2005). Consistent with our crosslinking results, when we modeled the protein docking of the C termini of DSP and OmpA, the linked lysine residues between the two proteins in the predicted model were within the crosslinker distance constraint for the BDP-NHP crosslinker (Figure S4B).

To validate this interaction, we immunoprecipitated DSP from Ab5075-infected H292 cells and uninfected H292 cells, and blotted for the presence of OmpA. OmpA precipitated with DSP from infected H292 cells in the presence and absence of crosslinker (Figures 5B and S4A), confirming the interaction observed through large-scale, in vivo crosslinking. Notably, two high-mass bands, both greater than 250,000 Da in size, were present only in the crosslinked sample (Figure S4A). These high molecular weight bands were presumed to be the crosslinked protein complex formed by DSP (>260 kDa) and OmpA (38 kDa). By confocal immunofluorescence, DSP and OmpA proteins co-localized during Ab5075 infection of H292 cells (Figure 6A). In addition, we observed an *A. baumannii* GUNK protein crosslinked with DSP. The GUNK identified in multiple peptide-peptide interactions with DSP was Ab57_2521 (later referred to as GUNK2), a signal-peptide-containing protein that also physically interacts with OmpA in infected host cells. The random chance of matching multiple interactors across species in this way was minuscule ($\rho = 2.35 \times 10^{-9}$, Figures 3B and S5A).

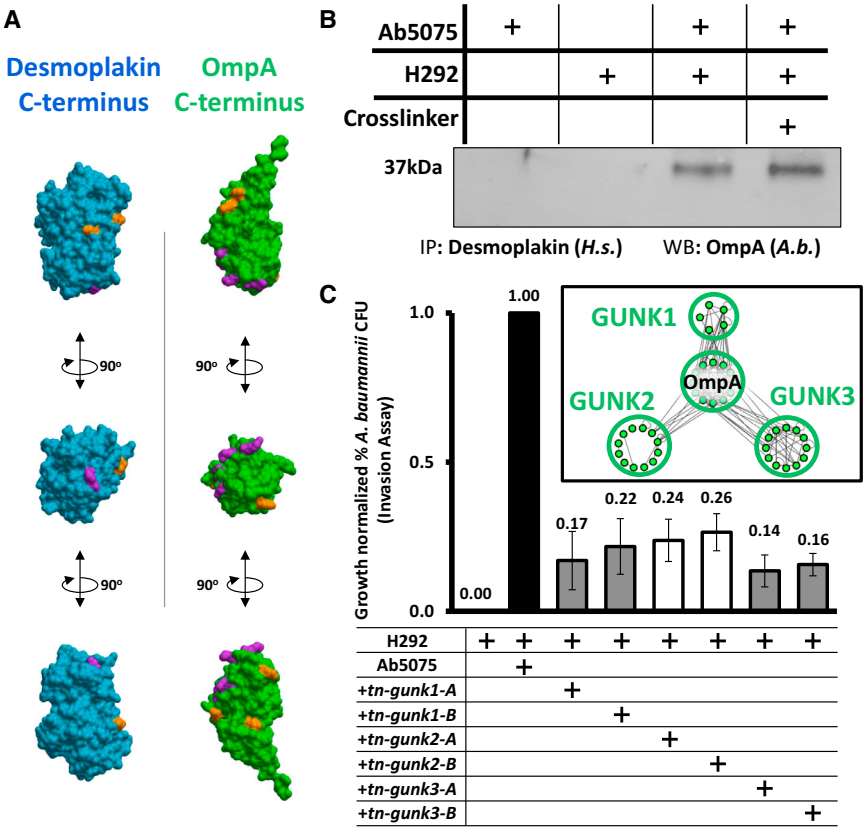

Figure 5. Functional Significance of Uncharacterized Interspecies Interactors and OmpA Interactors

(A) Space-filling models for crystal structures of OmpA (green, PDB: 4G4Y) and DSP (blue, PDB: 1LM5). Identified sites of crosslinking are highlighted in orange. Sites crosslinked between DSP and OmpA are highlighted in magenta.

(B) Immunoprecipitation (IP) of DSP from Ab5075 cells, H292 cells alone, or Ab5075-infected H292 cells (with and without crosslinker). H.s., *Homo sapiens*; A.b., *A. baumannii*; WB, western blot.

(C) Ab5075 invasion assays comparing WT Ab5075 with Ab5075 with transposon disruption mutants of GUNK1, GUNK2, and GUNK3 (Ab57_1108, Ab57_2521, and Ab57_2983). Mean ± SEM. Inset: crosslinked site interactions between GUNK proteins and OmpA from Ab5075 crosslinked alone (nodes: non-redundant crosslinked lysines; edges: crosslinked relationships).

Guilt by Association: Functional Significance of Genes of Unknown Function

Defining the function and biological significance of GUNK proteins remains a challenge (Meier et al., 2013). The unbiased determination of interactions between GUNK proteins and annotated gene products from a bacterial genome offers clues for putative functional characterization of GUNKs (Wang and Marcotte, 2010). In addition to crosslinking infected host cells, we harvested Ab5075 alone and crosslinked the bacterial cells to improve network and structural coverage of bacterial interprotein and intraprotein crosslinks within Ab5075 (Table S3). Of particular interest were GUNK proteins we observed linked to OmpA, since OmpA appears necessary for bacterial infection (Figure 4). In both infected host cells and *A. baumannii* cells alone, we observed crosslinks between OmpA and several GUNK proteins (Tables S1 and S3). We quantified bacterial invasion in host cells using transposon insertion mutants of three unannotated GUNKs most frequently identified as crosslinked to OmpA, hereafter GUNK1 (Ab57_1108), GUNK2 (Ab57_2521), and GUNK3 (Ab57_2983) (Figure 5C and Table S1). Transposon insertion mutants of GUNK1, GUNK2, and GUNK3 in the Ab5075 background showed reduced host cell invasion compared with WT Ab5075 (Figure 5C). Two independent transposon mutants (A and B) for each GUNK gene were tested and were observed to have consistent phenotypes (Figure 5C). While the attenuation of mutant bacterial invasion was not as great for these GUNK proteins as for OmpA, the reduction was still statistically significant compared with WT Ab5075 ($p < 2 \times 10^{-4}$, $p < 7 \times 10^{-5}$, and $p < 9 \times 10^{-7}$ for GUNK1, -2 and -3, respectively) (Figure 5C).

The Intersection of PPIs and Bacterial Genes Essential for Persistence in Host Lungs

We compared our dataset of interspecies crosslinked proteins with a recently established set of *A. baumannii* genes determined to be essential for bacterial persistence in the murine lung (Wang et al., 2014). Of the bacterial proteins we identified in crosslinked interspecies interactions (n = 31), we observed a significant enrichment of essential persistence genes (7/31, p = 0.000664) (Figure S5B). Discrepancies between these two datasets can in part be explained by three factors. First, a different, less virulent strain of *A. baumannii* (Ab17978) was used to test persistence in the murine lung (Jacobs et al., 2014; Wang et al., 2014). Second, not all proteins essential for invasion may interact with host proteins (proteins identified in persistence study but not in the proteomic interactome). Third, not all protein interactions between host and pathogen proteins may be essential (proteins identified in proteomic interactome but not in persistence study). Nonetheless, these results from in vivo host-pathogen crosslinking provide the first identification of host partners for seven *A. baumannii* proteins previously found to be essential for bacterial persistence in the host lung.

DISCUSSION

Interspecies protein interactions are critical determinants in bacterial infection and pathogenesis (Elde and Malik, 2009). Improved knowledge on which interspecies PPIs exist and how the involved proteins interact can greatly advance our understanding of molecular mechanisms involved in host invasion and provide new opportunities for antibacterial therapies. As the growing threat of antibiotic-resistant pathogens appears likely to surpass all currently known antibiotics (Davies and Davies, 2010; Blair et al., 2015), new knowledge and strategies that can help treat multidrug-resistant bacterial infections are of critical importance. Many strains of *A. baumannii*, such as

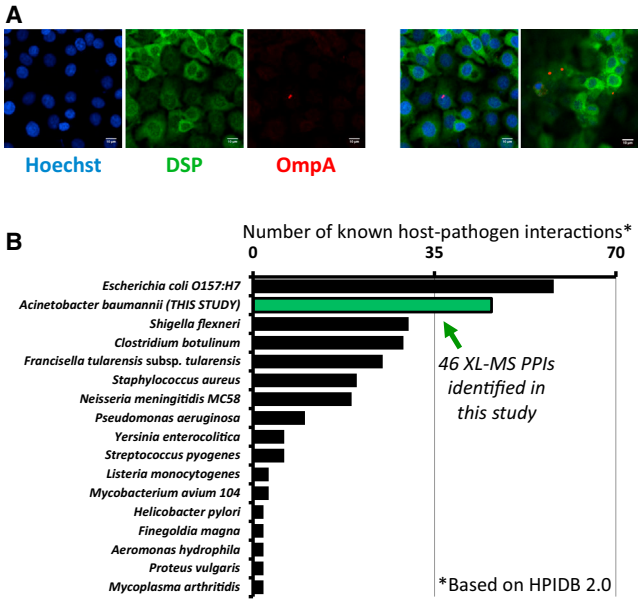

Figure 6. Ab5075 Host-Pathogen Interactions

(A) Confocal micrographs of Ab5075-infected H292 cells stained with primary antibodies against desmoplakin (green) and OmpA (red). DNA was stained with Hoechst 33,342 (blue). Confocal images and overlaid images from replicate analyses at a minimal thickness of 1.1 μm. Scale bars represent 10 μm.

(B) The 46 host-pathogen interactions identified in this study (green bar) compared with the number of interspecies interactions identified for other bacterial species (HPIDB 2.0 database) (Kumar and Nanduri, 2010). If substrains were present in the database, the strain with the highest number of interactions was shown. Due to scale, HPIDB 2.0 host-pathogen interactions for *Yersinia pestis* (n = 4,018), *Bacillus anthracis* (n = 3,061), and *Francisella tularensis* subsp. *tularensis* SCHU S4 (n = 1,346) are not shown.

the clinical strain Ab5075 used in these studies, exhibit increased resistance to all antibiotics, including carbapenems (Jacobs et al., 2014; Davies and Davies, 2010). Using unbiased in vivo protein crosslinking we identified physical interspecies PPIs during microbial infection to enable the first visualization of the *A. baumannii*-host interaction network. In total more than 3,000 crosslinked peptide pairs were identified, defining the existence and structural features of more than 700 PPIs and 46 interspecies PPIs, representing one of the largest host-bacteria protein interaction datasets and the first large-scale PPI analysis of host-pathogen interactions for *A. baumannii* (based on HPIDB2.0, Figure 6B) (Kumar and Nanduri, 2010).

Previous studies have shown the outer membrane protein OmpA to be critical to attachment and invasion in many pathogenic bacteria (Confer and Ayalew, 2013), including *A. baumannii* (Choi et al., 2008a; Jin et al., 2011). OmpA was also identified as a required gene for microbial persistence in murine lung infection ($\rho = 7.6 \times 10^{-79}$) (Wang et al., 2014). Although our experimental design did not specifically target OmpA, the membrane porin was identified in crosslinked relationships to several host proteins in infected epithelial cells. During infection OmpA migrates to at least three subcellular locations within host cells: mitochondria, nuclei, and cell surfaces (Lee et al., 2010; Choi et al., 2008b). Consistent with these findings, we identified OmpA interspecies interactions with a mitochondrial protein that affects reactive oxygen species generation (GFM-1) (Prasad et al., 2010; Soiferman et al., 2014), a nuclear protein involved in the DNA damage response (Salton et al., 2010) and circadian rhythm regulation (Guillaumond et al., 2011) (SFPQ), and the obligate desmosomal adhesion protein DSP (Figure 3B).

Bacterial targeting of adhesion complexes is a well-established mechanism for microbial intrusion and invasion (Guttman et al., 2006, 2007). Gram-negative bacteria, such as *Staphylococcus aureus* (Stanley and Amagai, 2006) and *Campylobacter jejuni* (Wine et al., 2008), have previously been observed to bind and disrupt desmosomes during infection. van Schilfgaarde et al. (1995) showed that bacterial intrusion into human lung epithelial cells placed infiltrating bacteria in close contact with desmosomal plaques. The in vivo crosslinking results presented here linking OmpA and DSP are consistent with these observations and are corroborated by the fact that OmpA co-localizes with DSP in infected human cells (Figure 6A). OmpA has previously been shown to be a component of secreted *A. baumannii* OMVs (Jin et al., 2011). OmpA and DSP could therefore co-localize after bacterial internalization (Rumbo et al., 2014) (Figures 4A and 6A) or through the local release of bacterial OMVs (Jin et al., 2011) and the subsequent integration of these vesicular membranes into the host membrane (Bomberger et al., 2009). For the latter case, altering desmosomal integrity could aid infiltration through host epithelia. Finally, because desmosomes integrate signals between the host cell surface and cytoskeleton (Green and Simpson, 2007), and a functional host cytoskeleton is required for *A. baumannii* pathogenesis (Rottner et al., 2005), binding and targeted disruption of the desmosome by bacterial proteins could be a means for *A. baumannii* to modulate the requisite host cytoskeleton and facilitate epithelial intrusion and host cell invasion. This speculation requires further investigation, of course, but knowledge of the OmpA-DSP interaction will enable these future studies.

With extensive evidence linking OmpA and orthologous proteins to pathogenicity, the discovery of GUNK proteins linked to OmpA established a preliminary association between these GUNKs and bacterial invasion. While two GUNK proteins were *A. baumannii* specific (GUNK2 and GUNK3), GUNK1 shares sequence identity with hypothetical proteins from *Bacillus* (52%) and *Pseudomonas* (43%) species and META-domain/HslJ proteins from *Bordetella* (38%) and *E. coli* (32%). The HslJ protein has previously been related to antibiotic resistance to novobiocin (Lilic et al., 2003), and overexpression of META proteins in *Leishmania* resulted in increased virulence (Uliana et al., 1999); META-domain proteins, often observed in hypothetical bacterial proteins (Ramos et al., 2004), have also been implicated in bacterial motility. The determination of multiple crosslinked relationships with OmpA provided interaction-based evidence (“guilt by association” [Wang and Marcotte, 2010]), leading to further characterization of these GUNK proteins. We believe that sequence similarity potentiating the involvement of GUNK1 in motility/resistance and the attenuated host invasion by all three GUNK transposon insertion mutants (Figure 5C) further support these GUNK proteins as putative *A. baumannii* virulence factors. These findings established the utility of an unbiased approach to identify novel interactions and disseminate

functional characterization from PPIs between known virulence factors and GUNK proteins.

The techniques underlying our study of in vivo protein crosslinking in bacterially infected human cells provide a unique opportunity to view networks of intercellular PPIs. Recent studies have suggested that interactomes, even incomplete ones, can enable discovery of molecular commonalities between phenotypically related disease pathologies that may not share primary disease genes (Menche et al., 2015). When extrapolated to the study of bacterial pathogenesis, overlapping interspecies interactomes could reveal common paradigms of infection exploited by microbes. In vivo crosslinking of host-pathogen systems is a generally applicable technology, and future applications with other pathogens will help to explore the possibility of common strategies used among multiple pathogens.

SIGNIFICANCE

Protein interactions are essential mediators of bacterial pathogenesis. While methods to elucidate bacterial proteins required for infection have been employed extensively, information regarding the host proteins targeted by bacteria and interspecies complex structures has been more difficult to determine. In this proof-of-principle study, we used chemical crosslinking of proteins in combination with large-scale MS to identify interspecies interactions between proteins in cultured human cells and Gram-negative bacterial proteins during bacterial infection. These efforts resulted in identification of interspecies PPIs between human proteins and known bacterial virulence factors. Most notably we identified bacterial virulence factors interacting with host structural proteins that mediate host cell-to-cell adhesion. Our study shows the potential of chemical crosslinking of proteins in combination with large-scale MS to shed new light on host-pathogen protein interactions and their structural features. We demonstrate the ability of said methods to interrogate protein interactions underlying complex pathogenic systems, and the presented methodologies are generally applicable to other pathogen systems. The broad application of these methods could aid the rapid expansion of understanding of how diverse bacterial species target and manipulate host proteins during pathogenesis.

EXPERIMENTAL PROCEDURES

Cell Culture

Ab5075 cells were grown to stationary phase in nutrient broth (BD). H292 cells were grown in RPMI-1640 (Thermo) with 10% fetal bovine serum and 1% penicillin/streptomycin (37°C, 5% CO_2). Transposon mutants in Ab5075 were attained from Dr. Colin Manoil (Gallagher et al., 2015).

Crosslinker Synthesis, Infection, Stage-1 Database Creation, and Sample Preparation

Biotin-aspartate proline-PIR *n*-hydroxyphthalimide (BDP-NHP) was synthesized as previously described (Weisbrod et al., 2013; Tang and Bruce, 2010). Confluent H292 cells were washed, released, and pelleted before resuspension in crosslinking (XL) buffer (0.17 M potassium phosphate) containing Ab5075 cells at a multiplicity of infection (MOI) of 500 for 2 hr. Five experiments were run: three biological replicates of Ab5075-infected H292 cells (Figure S6) and two biological replicates of uninfected H292 cells (Table S2). BDP-NHP (8 mM) was added to the cell suspension for 1 hr. H292 cells infected with *A. baumannii* (i.e., HA-1, HA-2, HA-3) and uninfected cells were washed, pelleted, and frozen at −80°C.

Infected H292 cell pellets were resuspended in lysis buffer: 8 M urea, 100 mM Tris-Cl (pH 8.0), 150 mM NaCl, and protease inhibitor tablets (Roche); then lysed by cryogrinding and sonication. Proteins were reduced and alkylated. Protein lysates were diluted with 100 mM Tris-Cl (pH 8.0). 1 mg of protein was removed to enrich full-length crosslinked proteins with monomeric avidin beads. Enriched, crosslinked proteins were digested with sequencing grade trypsin (Promega), and injected on a C-8 column eluting into an LTQ-XL or LTQ-Velos-FT-ICR mass spectrometer to create a search database of proteins that had been crosslinked (stage-1 database) (Weisbrod et al., 2013). Digested stage-1 peptide samples were shot in quadruplicate on a 4-hr reverse-phase data-dependent Top5 method. Spectra were searched using SEQUEST. 30,880 peptide-spectral matches (10,304 unique peptides) were identified at an FDR of less than 1%, based on a concatenated, target-decoy database of all human and *A. baumannii* (AB0057) proteins (Weisbrod et al., 2013). The remaining protein lysates were digested with sequencing grade trypsin. Digested peptides were desalted and fractionated by strong cation exchange. Eluted peptides were incubated with monomeric avidin beads to enrich crosslinked peptides.

Liquid Chromatography-MS/MS/MS, ReACT, Database Searching, and Data Analysis

Crosslinked peptides were resuspended in 5% acetonitrile/2% formic acid and injected onto an in-house pulled C-8 column (Magic, 200 A, 5 μm) run on 4-hr gradients as with the stage-1 mass spectral analysis; eluted peptides were analyzed on an LTQ-Velos-FT-ICR. Crosslinked peptides were fragmented in a data-dependent ReACT mode (Real-time Analysis for Crosslinked peptide Technology) (Weisbrod et al., 2013). In brief, high-charge state precursor ions (MS^1, $z > 4+$) were isolated and fragmented at low energy ($Q = 0.20$) to release crosslinked peptides and a reporter ion ($m/z = 752.41$). Data-dependent selection of fragmented MS^2 ions that sum to the precursor mass minus the reporter ion were further fragmented for MS^3 spectra and peptide sequencing.

All parameters and filtering were done as previously described to identify unique PPIs and site-site interactions (Weisbrod et al., 2013). The final relationship FDR was calculated to be 0.24% [(2 × 20 decoy relationships with at least one reverse hit)/16,758 total relationships]. The final PPI FDR was 1% [(2 × 4 unique decoy PPIs)/719 total unique PPIs]. All interaction data, including pep.xml files, can be found at http://brucelab.gs.washington.edu/xlinkdb/. Protein interaction networks were created using Cytoscape 3.0. Protein structures for OmpA and desmoplakin were downloaded from the PDB (PDB: 4G4Y and 1LM5, respectively). Protein structure interactions were modeled using PatchDock (Schneidman-Duhovny et al., 2005). KEGG pathway enrichment p values were determined using STRING v9.1 (Franceschini et al., 2013).

Gentamicin Protection Assays

H292 cells were plated in 24-well plates and allowed to attach for 16 hr. H292 were incubated with Ab5075 or Ab5075-*tn-ompa* for 3 hr in serum-free, antibiotic-free RPMI-1640 medium (RPMI). The supernatant was saved to normalize Ab5075 growth during infection. H292 cells were incubated for 1 hr with 200 μg/ml gentamicin in RPMI at 37°C. Lysis buffer (PBS with 0.1% Triton X-100) was added to each well, and the plate was shaken at 200 rpm for 10 min. Lysates (50 μl) were cultured on NB-agar plates (16 hr, 37°C). Colonies were counted and normalized to WT Ab5075 growth. Values are the average of technical duplicates from at least three experiments performed on three different days. For antibody blocking of OmpA-based invasion, Ab5075 cells were pre-incubated with α-OmpA or PBS-control serum (Dr. Michael McConnell) or purified Genscript synthesized antibodies. Pre-treated Ab5075 cells were then incubated with H292 cells as described above.

Confocal Immunofluorescence and Brightfield Microscopy

Confluent H292 cells were infected with Ab5075 (MOI = 100) on 3.5-cm plates with glass coverslips (No. 1.5, Mattek). For confocal immunofluorescence, cells were fixed (formalin), blocked (3% milk in PBS with Tween 20), and incubated overnight at 4°C with α-DSP antibody (rabbit, Abcam) and primary mouse α-OmpA serum (Dr. Michael McConnell) in blocking buffer. Microscopy was performed with a Nikon A1 confocal mounted on a Nikon TiE inverted

microscope (Garvey Cell Imaging Lab) at 20× magnification, n = 1 (air), NA = 0.75. Depth of field was measured based on λ = 595 nm. For brightfield microscopy, H292 cells were grown to confluency on 24-well plates, incubated in crosslinking buffer ± Ab5075 cells (MOI = 100), washed with PBS, and imaged at 20× magnification.

Murine Acute Lung Infection

WT Ab5075 or *tn-ompA* were streaked on LB agar or LB agar with 5 μg/ml tetracycline (LBtet) from frozen stocks. PBS (50 μl) containing ~2 × 10^8 cfu/ml bacteria were administered intratracheally to anesthetized mice as described previously (Kaneko et al., 2007). Animals that became moribund or distressed, or were unable to eat or drink were euthanized using a CO_2 chamber. Experiments were approved by the University of Washington Institutional Animal Care and Use Committee (protocol number 4113-01).

Co-immunoprecipitation and Western Blotting

H292 cells were grown to confluency and washed prior to co-incubation with Ab5075 cells (MOI = 500) for 2 hr at room temperature. Subsequently, either DMSO or BDP-NHP in DMSO was added to the samples followed by 1 hr of incubation. Cells were pelleted and resuspended in immunoprecipitation (IP) buffer (10 mM Tris-Cl [pH 8.0], 100 mM NaCl, 1% Triton X-100, 1 mM EDTA, protease inhibitors, 100 μg/ml lysozyme) and incubated on ice for 30 min to lyse bacterial cells; samples were syringe pumped (27.5-gauge needle) and sonicated to further lyse cells and fragment DNA.

Lysates were pre-cleared with 50 μl of protein G agarose (Thermo) mixed at 4°C for 1 hr. α-Desmoplakin antibody was added for 16.5 hr at 4°C. For immunoprecipitation, 50 μl of protein G agarose was added for 3 hr at 4°C. Beads were pelleted and thoroughly washed. Co-IP proteins were eluted at 95°C for 10 min with a 3:1 ratio of 1% SDS, 15% glycerol, 50 mM Tris-Cl (pH 8.0), 150 mM NaCl: XT Sample Buffer (Bio-Rad). Finally, proteins were detected by SDS-PAGE and western blot (primary: α-OmpA serum; secondary: α-mouse antibodies [IRDye, Li-Cor]).

Further descriptions of protocols can be found in the Supplemental Experimental Procedures.

SUPPLEMENTAL INFORMATION

Supplemental Information includes Supplemental Experimental Procedures, three tables, and six figures and can be found with this article online at http://dx.doi.org/10.1016/j.chembiol.2015.09.015.

ACKNOWLEDGMENTS

This work was supported by NIH grants U19-AI107775-02 (J.E.B. and C.M.), R01-AI101307-03 (P.K.S., J.E.B., and C.M.), R01-GM086688-06 (J.E.B.), and R01-HL110879-04 (P.K.S. and J.E.B.).The authors thank Chunxiang Zheng and Jimmy Eng, and Drs. Arti Navare and Priska von Haller for advice concerning experimentation, technology, and programming; Dr. Nicholas Foti for help with statistical analyses; Drs. Rustin Lovewell and Brent Berwin for advice concerning bacterial invasion assays; Dr. Michael McConnell for control and α-OmpA serum; and Dr. Ron Seifert (UW Garvey Cell Imaging Lab) for assistance with microscopy.

Received: June 9, 2015
Revised: September 11, 2015
Accepted: September 24, 2015
Published: November 5, 2015

REFERENCES

Barber, M.F., and Elde, N.C. (2014). Nutritional immunity. Escape from bacterial iron piracy through rapid evolution of transferrin. Science *346*, 1362–1366.

Beck, M., Schmidt, A., Malmstroem, J., Claassen, M., Ori, A., Szymborska, A., Herzog, F., Rinner, O., Ellenberg, J., and Aebersold, R. (2011). The quantitative proteome of a human cell line. Mol. Syst. Biol. *7*, 549.

Blair, J.M., Webber, M.A., Baylay, A.J., Ogbolu, D.O., and Piddock, L.J. (2015). Molecular mechanisms of antibiotic resistance. Nat. Rev. Microbiol. *13*, 42–51.

Bomberger, J.M., Maceachran, D.P., Coutermarsh, B.A., Ye, S., O'Toole, G.A., and Stanton, B.A. (2009). Long-distance delivery of bacterial virulence factors by *Pseudomonas aeruginosa* outer membrane vesicles. PLoS Pathog. *5*, e1000382.

Carpenter, E.P., Beis, K., Cameron, A.D., and Iwata, S. (2008). Overcoming the challenges of membrane protein crystallography. Curr. Opin. Struct. Biol. *18*, 581–586.

Chavez, J.D., Hoopmann, M.R., Weisbrod, C.R., Takara, K., and Bruce, J.E. (2011). Quantitative proteomic and interaction network analysis of cisplatin resistance in HeLa cells. PLoS One *6*, e19892.

Choi, H.J., Park-Snyder, S., Pascoe, L.T., Green, K.J., and Weis, W.I. (2002). Structures of two intermediate filament-binding fragments of desmoplakin reveal a unique repeat motif structure. Nat. Struct. Biol. *9*, 612–620.

Choi, C.H., Lee, J.S., Lee, Y.C., Park, T.I., and Lee, J.C. (2008a). *Acinetobacter baumannii* invades epithelial cells and outer membrane protein A mediates interactions with epithelial cells. BMC Microbiol. *8*, 216.

Choi, C.H., Hyun, S.H., Lee, J.Y., Lee, J.S., Lee, Y.S., Kim, S.A., Chae, J.P., Yoo, S.M., and Lee, J.C. (2008b). *Acinetobacter baumannii* outer membrane protein A targets the nucleus and induces cytotoxicity. Cell Microbiol. *10*, 309–319.

Confer, A.W., and Ayalew, S. (2013). The OmpA family of proteins: roles in bacterial pathogenesis and immunity. Vet. Microbiol. *163*, 207–222.

Cossart, P., and Lecuit, M. (1998). Interactions of *Listeria monocytogenes* with mammalian cells during entry and actin-based movement: bacterial factors, cellular ligands and signaling. EMBO J. *17*, 3797–3806.

Cossart, P., and Sansonetti, P.J. (2004). Bacterial invasion: the paradigms of enteroinvasive pathogens. Science *304*, 242–248.

Davies, J., and Davies, D. (2010). Origins and evolution of antibiotic resistance. Microbiol. Mol. Biol. Rev. *74*, 417–433.

Delva, E., Tucker, D.K., and Kowalczyk, A.P. (2009). The desmosome. Cold Spring Harb. Perspect. Biol. *1*, a002543.

Demogines, A., Abraham, J., Choe, H., Farzan, M., and Sawyer, S.L. (2013). Dual host-virus arms races shape an essential housekeeping protein. PLoS Biol. *11*, e1001571.

Elde, N.C., and Malik, H.S. (2009). The evolutionary conundrum of pathogen mimicry. Nat. Rev. Microbiol. *7*, 787–797.

Elde, N.C., Child, S.J., Geballe, A.P., and Malik, H.S. (2009). Protein kinase R reveals an evolutionary model for defeating viral mimicry. Nature *457*, 485–489.

Fields, S., and Song, O. (1989). A novel genetic system to detect protein-protein interactions. Nature *340*, 245–246.

Franceschini, A., Szklarczyk, D., Frankild, S., Kuhn, M., Simonovic, M., Roth, A., Lin, J., Minguez, P., Bork, P., von Mering, C., et al. (2013). STRING v9.1: protein-protein interaction networks, with increased coverage and integration. Nucleic Acids Res. *41*, D808–D815.

Galdiero, S., Falanga, A., Cantisani, M., Tarallo, R., Della Pepa, M.E., D'Oriano, V., and Galdiero, M. (2012). Microbe-host interactions: structure and role of Gram-negative bacterial porins. Curr. Protein Pept. Sci. *13*, 843–854.

Gallagher, L.A., Ramage, E., Weiss, E.J., Radey, M., Hayden, H.S., Held, K.G., Huse, H.K., Zurawski, D.V., Brittnacher, M.J., and Manoil, C. (2015). Resources for genetic and genomic analysis of emerging pathogen *Acinetobacter baumannii*. J. Bacteriol. *197*, 2027–2035.

Garrod, D., and Chidgey, M. (2008). Desmosome structure, composition and function. Biochim. Biophys. Acta *1778*, 572–587.

Gingras, A.C., Gstaiger, M., Raught, B., and Aebersold, R. (2007). Analysis of protein complexes using mass spectrometry. Nature reviews. Mol. Cell Biol. *8*, 645–654.

Green, K.J., and Simpson, C.L. (2007). Desmosomes: new perspectives on a classic. J. Invest. Dermatol. *127*, 2499–2515.

Guillaumond, F., Boyer, B., Becquet, D., Guillen, S., Kuhn, L., Garin, J., Belghazi, M., Bosler, O., Franc, J.L., and Francois-Bellan, A.M. (2011). Chromatin remodeling as a mechanism for circadian prolactin transcription: rhythmic NONO and SFPQ recruitment to HLTF. FASEB J. *25*, 2740–2756.

Guttman, J.A., Li, Y., Wickham, M.E., Deng, W., Vogl, A.W., and Finlay, B.B. (2006). Attaching and effacing pathogen-induced tight junction disruption in vivo. Cell Microbiol. *8*, 634–645.

Guttman, J.A., Kazemi, P., Lin, A.E., Vogl, A.W., and Finlay, B.B. (2007). Desmosomes are unaltered during infections by attaching and effacing pathogens. Anat. Rec. (Hoboken) *290*, 199–205.

Herzog, F., Kahraman, A., Boehringer, D., Mak, R., Bracher, A., Walzthoeni, T., Leitner, A., Beck, M., Hartl, F.U., Ban, N., et al. (2012). Structural probing of a protein phosphatase 2A network by chemical cross-linking and mass spectrometry. Science *337*, 1348–1352.

Jacobs, A.C., Thompson, M.G., Black, C.C., Kessler, J.L., Clark, L.P., McQueary, C.N., Gancz, H.Y., Corey, B.W., Moon, J.K., Si, Y., et al. (2014). AB5075, a highly virulent isolate of *Acinetobacter baumannii*, as a model strain for the evaluation of pathogenesis and antimicrobial treatments. MBio *5*, e01076–01014.

Jager, S., Cimermancic, P., Gulbahce, N., Johnson, J.R., McGovern, K.E., Clarke, S.C., Shales, M., Mercenne, G., Pache, L., Li, K., et al. (2012). Global landscape of HIV-human protein complexes. Nature *481*, 365–370.

Jin, J.S., Kwon, S.O., Moon, D.C., Gurung, M., Lee, J.H., Kim, S.I., and Lee, J.C. (2011). *Acinetobacter baumannii* secretes cytotoxic outer membrane protein A via outer membrane vesicles. PLoS One *6*, e17027.

Kaake, R.M., Wang, X., Burke, A., Yu, C., Kandur, W., Yang, Y., Novtisky, E.J., Second, T., Duan, J., Kao, A., et al. (2014). A new in vivo cross-linking mass spectrometry platform to define protein-protein interactions in living cells. Mol. Cell. Proteomics *13*, 3533–3543.

Kaneko, Y., Thoendel, M., Olakanmi, O., Britigan, B.E., and Singh, P.K. (2007). The transition metal gallium disrupts *Pseudomonas aeruginosa* iron metabolism and has antimicrobial and antibiofilm activity. J. Clin. Invest. *117*, 877–888.

Kelley, L.A., and Sternberg, M.J. (2009). Protein structure prediction on the Web: a case study using the Phyre server. Nat. Protoc. *4*, 363–371.

Kumar, R., and Nanduri, B. (2010). HPIDB—a unified resource for host-pathogen interactions. BMC Bioinformatics *11* (*Suppl 6*), S16.

Kwon, S.O., Gho, Y.S., Lee, J.C., and Kim, S.I. (2009). Proteome analysis of outer membrane vesicles from a clinical *Acinetobacter baumannii* isolate. FEMS Microbiol. Lett. *297*, 150–156.

Lee, J.S., Choi, C.H., Kim, J.W., and Lee, J.C. (2010). *Acinetobacter baumannii* outer membrane protein A induces dendritic cell death through mitochondrial targeting. J. Microbiol. *48*, 387–392.

Lievin-Le Moal, V., and Servin, A.L. (2006). The front line of enteric host defense against unwelcome intrusion of harmful microorganisms: mucins, antimicrobial peptides, and microbiota. Clin. Microbiol. Rev. *19*, 315–337.

Lilic, M., Jovanovic, M., Jovanovic, G., and Savic, D.J. (2003). Identification of the CysB-regulated gene, hslJ, related to the *Escherichia coli* novobiocin resistance phenotype. FEMS Microbiol. Lett. *224*, 239–246.

Marcoux, J., Politis, A., Rinehart, D., Marshall, D.P., Wallace, M.I., Tamm, L.K., and Robinson, C.V. (2014). Mass spectrometry defines the C-terminal dimerization domain and enables modeling of the structure of full-length OmpA. Structure *22*, 781–790.

McConnell, M.J., Actis, L., and Pachon, J. (2013). *Acinetobacter baumannii*: human infections, factors contributing to pathogenesis and animal models. FEMS Microbiol. Rev. *37*, 130–155.

Meier, M., Sit, R.V., and Quake, S.R. (2013). Proteome-wide protein interaction measurements of bacterial proteins of unknown function. Proc. Natl. Acad. Sci. USA *110*, 477–482.

Menche, J., Sharma, A., Kitsak, M., Ghiassian, S.D., Vidal, M., Loscalzo, J., and Barabasi, A.L. (2015). Disease networks. Uncovering disease-disease relationships through the incomplete interactome. Science *347*, 1257601.

Navare, A.T., Chavez, J.D., Zheng, C., Weisbrod, C.R., Eng, J.K., Siehnel, R., Singh, P.K., Manoil, C., and Bruce, J.E. (2015). Probing the protein interaction network of *Pseudomonas aeruginosa* cells by chemical cross-linking mass spectrometry. Structure *23*, 762–773.

Nekrasova, O., and Green, K.J. (2013). Desmosome assembly and dynamics. Trends Cell Biol. *23*, 537–546.

Okuda, J., Hayashi, N., Okamoto, M., Sawada, S., Minagawa, S., Yano, Y., and Gotoh, N. (2010). Translocation of *Pseudomonas aeruginosa* from the intestinal tract is mediated by the binding of ExoS to an Na,K-ATPase regulator, FXYD3. Infect. Immun. *78*, 4511–4522.

Orchard, S., Ammari, M., Aranda, B., Breuza, L., Briganti, L., Broackes-Carter, F., Campbell, N.H., Chavali, G., Chen, C., del-Toro, N., et al. (2014). The MIntAct project—IntAct as a common curation platform for 11 molecular interaction databases. Nucleic Acids Res. *42*, D358–D363.

Park, J.S., Lee, W.C., Yeo, K.J., Ryu, K.S., Kumarasiri, M., Hesek, D., Lee, M., Mobashery, S., Song, J.H., Kim, S.I., et al. (2012). Mechanism of anchoring of OmpA protein to the cell wall peptidoglycan of the gram-negative bacterial outer membrane. FASEB J. *26*, 219–228.

Patel, M.R., Loo, Y.M., Horner, S.M., Gale, M., Jr., and Malik, H.S. (2012). Convergent evolution of escape from hepaciviral antagonism in primates. PLoS Biol. *10*, e1001282.

Peterson, L.W., and Artis, D. (2014). Intestinal epithelial cells: regulators of barrier function and immune homeostasis. Nat. Rev. Immunol. *14*, 141–153.

Petersen, T.N., Brunak, S., von Heijne, G., and Nielsen, H. (2011). SignalP 4.0: discriminating signal peptides from transmembrane regions. Nat. Methods *8*, 785–786.

Petrotchenko, E.V., and Borchers, C.H. (2010). Crosslinking combined with mass spectrometry for structural proteomics. Mass Spectrom. Rev. *29*, 862–876.

Prasad, T., Hameed, S., Manoharlal, R., Biswas, S., Mukhopadhyay, C.K., Goswami, S.K., and Prasad, R. (2010). Morphogenic regulator EFG1 affects the drug susceptibilities of pathogenic *Candida albicans*. FEMS Yeast Res. *10*, 587–596.

Ramos, C.S., Franco, F.A., Smith, D.F., and Uliana, S.R. (2004). Characterisation of a new *Leishmania* META gene and genomic analysis of the META cluster. FEMS Microbiol. Lett. *238*, 213–219.

Rinner, O., Seebacher, J., Walzthoeni, T., Mueller, L.N., Beck, M., Schmidt, A., Mueller, M., and Aebersold, R. (2008). Identification of cross-linked peptides from large sequence databases. Nat. Methods *5*, 315–318.

Rottner, K., Stradal, T.E., and Wehland, J. (2005). Bacteria-host-cell interactions at the plasma membrane: stories on actin cytoskeleton subversion. Dev. Cell *9*, 3–17.

Rumbo, C., Tomas, M., Fernandez Moreira, E., Soares, N.C., Carvajal, M., Santillana, E., Beceiro, A., Romero, A., and Bou, G. (2014). The *Acinetobacter baumannii* Omp33-36 porin is a virulence factor that induces apoptosis and modulates autophagy in human cells. Infect. Immun. *82*, 4666–4680.

Salton, M., Lerenthal, Y., Wang, S.Y., Chen, D.J., and Shiloh, Y. (2010). Involvement of Matrin 3 and SFPQ/NONO in the DNA damage response. Cell Cycle *9*, 1568–1576.

Schneidman-Duhovny, D., Inbar, Y., Nussinov, R., and Wolfson, H.J. (2005). PatchDock and SymmDock: servers for rigid and symmetric docking. Nucleic Acids Res. *33*, W363–W367.

Shapira, S.D., Gat-Viks, I., Shum, B.O., Dricot, A., de Grace, M.M., Wu, L., Gupta, P.B., Hao, T., Silver, S.J., Root, D.E., et al. (2009). A physical and regulatory map of host-influenza interactions reveals pathways in H1N1 infection. Cell *139*, 1255–1267.

Soiferman, D., Ayalon, O., Weissman, S., and Saada, A. (2014). The effect of small molecules on nuclear-encoded translation diseases. Biochimie *100*, 184–191.

Sowa, M.E., Bennett, E.J., Gygi, S.P., and Harper, J.W. (2009). Defining the human deubiquitinating enzyme interaction landscape. Cell *138*, 389–403.

Stanley, J.R., and Amagai, M. (2006). Pemphigus, bullous impetigo, and the staphylococcal scalded-skin syndrome. N. Engl. J. Med. *355*, 1800–1810.

Subbotin, R.I., and Chait, B.T. (2014). A pipeline for determining protein-protein interactions and proximities in the cellular milieu. Mol. Cell. Proteomics *13*, 2824–2835.

Swanson, J.A., and Baer, S.C. (1995). Phagocytosis by zippers and triggers. Trends Cell Biol. *5*, 89–93.

Tang, X., and Bruce, J.E. (2010). A new cross-linking strategy: protein interaction reporter (PIR) technology for protein-protein interaction studies. Mol. Biosyst. *6*, 939–947.

Tang, X.T., Munske, G.R., Siems, W.F., and Bruce, J.E. (2005). Mass spectrometry identifiable cross-linking strategy for studying protein-protein interactions. Anal. Chem. *77*, 311–318.

Tang, X., Yi, W., Munske, G.R., Adhikari, D.P., Zakharova, N.L., and Bruce, J.E. (2007). Profiling the membrane proteome of *Shewanella oneidensis* MR-1 with new affinity labeling probes. J. Proteome Res. *6*, 724–734.

Tarassov, K., Messier, V., Landry, C.R., Radinovic, S., Serna Molina, M.M., Shames, I., Malitskaya, Y., Vogel, J., Bussey, H., and Michnick, S.W. (2008). An in vivo map of the yeast protein interactome. Science *320*, 1465–1470.

Tosi, A., Haas, C., Herzog, F., Gilmozzi, A., Berninghausen, O., Ungewickell, C., Gerhold, C.B., Lakomek, K., Aebersold, R., Beckmann, R., et al. (2013). Structure and subunit topology of the INO80 chromatin remodeler and its nucleosome complex. Cell *154*, 1207–1219.

Uliana, S.R., Goyal, N., Freymuller, E., and Smith, D.F. (1999). *Leishmania*: overexpression and comparative structural analysis of the stage-regulated meta 1 gene. Exp. Parasitol. *92*, 183–191.

van Schilfgaarde, M., van Alphen, L., Eijk, P., Everts, V., and Dankert, J. (1995). Paracytosis of *Haemophilus influenzae* through cell layers of NCI-H292 lung epithelial cells. Infect. Immun. *63*, 4729–4737.

Wang, P.I., and Marcotte, E.M. (2010). It's the machine that matters: predicting gene function and phenotype from protein networks. J. Proteomics *73*, 2277–2289.

Wang, N., Ozer, E.A., Mandel, M.J., and Hauser, A.R. (2014). Genome-wide identification of *Acinetobacter baumannii* genes necessary for persistence in the lung. MBio *5*, e01163–01114.

Weisbrod, C.R., Chavez, J.D., Eng, J.K., Yang, L., Zheng, C., and Bruce, J.E. (2013). In vivo protein interaction network identified with a novel real-time cross-linked peptide identification strategy. J. Proteome Res. *12*, 1569–1579.

Wine, E., Chan, V.L., and Sherman, P.M. (2008). *Campylobacter jejuni* mediated disruption of polarized epithelial monolayers is cell-type specific, time dependent, and correlates with bacterial invasion. Pediatr. Res. *64*, 599–604.

Yang, B., Wu, Y.J., Zhu, M., Fan, S.B., Lin, J., Zhang, K., Li, S., Chi, H., Li, Y.X., Chen, H.F., et al. (2012). Identification of cross-linked peptides from complex samples. Nat. Methods *9*, 904–906.

Zarantonelli, M.L., Szatanik, M., Giorgini, D., Hong, E., Huerre, M., Guillou, F., Alonso, J.M., and Taha, M.K. (2007). Transgenic mice expressing human transferrin as a model for meningococcal infection. Infect. Immun. *75*, 5609–5614.

Zhang, H., Tang, X., Munske, G.R., Tolic, N., Anderson, G.A., and Bruce, J.E. (2009). Identification of protein-protein interactions and topologies in living cells with chemical cross-linking and mass spectrometry. Mol. Cell. Proteomics *8*, 409–420.

Zhang, Q.C., Petrey, D., Garzon, J.I., Deng, L., and Honig, B. (2013). PrePPI: a structure-informed database of protein-protein interactions. Nucleic Acids Res. *41*, D828–D833.

Zheng, C., Yang, L., Hoopmann, M.R., Eng, J.K., Tang, X., Weisbrod, C.R., and Bruce, J.E. (2011). Cross-linking measurements of in vivo protein complex topologies. Mol. Cell. Proteomics *10*, M110 006841.

Zheng, C., Weisbrod, C.R., Chavez, J.D., Eng, J.K., Sharma, V., Wu, X., and Bruce, J.E. (2013). XLink-DB: database and software tools for storing and visualizing protein interaction topology data. J. Proteome Res. *12*, 1989–1995.

Zybailov, B.L., Glazko, G.V., Jaiswal, M., and Raney, K.D. (2013). Large scale chemical cross-linking mass spectrometry perspectives. J. Proteomics Bioinform. *6*, 001.

